Kinetics of the processes of desorption from fatty acid monolayers

Gajanan S. Patil, Richard H. Matthews, and David G. Cornwell

Department of Physiological Chemistry, The Ohio State University, Columbus, Ohio 43210

Abstract The surface area, A, of contracting fatty acid monolayers was measured as a function of time, t, at constant surface pressure. In the initial temporal phase, ln A was linear with $\sqrt{t}$. In a subsequent steady-state phase, ln A was linear with t. The initial desorption coefficient for sodium palmitate, K_t, and the steady-state desorption coefficient, K_s, varied directly with surface pressure and subphase pH, and these desorption coefficients also varied with the composition of the subphase buffer. However, the K_s/K_t ratio was independent of these variables. The diffusion coefficient, D_{25}, for sodium palmitate calculated from desorption coefficient ratios was $4.8 \pm 0.6 \times 10^{-6}$ cm^2/sec. This value was in reasonable agreement with D_{25} for sodium palmitate measured by time-lag diffusion, $3.7 \pm 0.6 \times 10^{-6}$ cm^2/sec. D_{25} values obtained for a series of fatty acids suggested that higher members of the series diffused as small aggregates averaging two to four molecules in size. Kinetic and diffusion data both supported a model for the desorption process described by Ter Minassian-Saraga.

Supplementary key words lauric acid · myristic acid · palmitic acid · palmitoleic acid · oleic acid · surface pressure · subphase pH · buffer composition · time-lag diffusion · diffusion coefficient · apparent surface pK_a

Monolayers that contain slightly soluble surface-active compounds such as lauric acid or myristic acid decrease in surface area when they are maintained at constant surface pressure (1) and demonstrate unusually small surface areas when their force–area curves are generated at a low compression rate (2). The decrease in area is usually explained by desorption from the monolayer into the aqueous subphase. The kinetics of the desorption process have been studied by several investigators. Ter Minassian-Saraga (3, 4) examined lauric acid monolayers and found that desorption was described by two temporal phases. The initial phase was represented by the equation:

$$K_t = -\frac{d \ln A}{d\sqrt{t}} \qquad \text{Eq. 1}$$

where A is the film area, t is time, and K_t is a coefficient which is a function of the diffusion coefficient D. A subsequent steady-state phase was described by the equation:

$$K_s = -\frac{d \ln A}{dt} \qquad \text{Eq. 2}$$

where K_s is a second coefficient which is a function of D. The desorption kinetics described by the Ter Minassian-Saraga model have been used to measure activity coefficients of substances in monolayers (5), cohesive forces in monolayers (6), the enzymatic hydrolysis of phospholipid monolayers (7), and the surface area per molecule in unstable desorbing films (6, 8).

Motomura et al. (2) recently described an equation of state for desorbing myristic acid monolayers and as a consequence of this study they developed a kinetic model for the desorption process (9) which differed significantly from the model developed by Ter Minassian-Saraga (3, 4). While Ter Minassian-Saraga found that ln A was initially linear with $\sqrt{t}$ (Eq. 1) and subsequently linear with t (Eq. 2), Matuura, Sekita, and Motomura (9) found that ln A was initially linear with t and subsequently linear with $\sqrt{t}$.

In the present investigation, we have examined the kinetics of the desorption process with palmitic acid. Desorption was studied at two surface pressures, and the palmitic acid was spread on several subphase buffers because desorption rates were functions of both surface pressure and the subphase buffer. The kinetic models for the desorption process developed by Ter Minassian-Saraga (3, 4) and Matuura et al. (9) both estimate the diffusion coefficient, D, for the desorbing species. We have, therefore, compared D calculated by Ter Minassian-Saraga (3, 4) and Matuura et al. (9) from desorption data and D calculated from our desorption data with

D obtained by an independent time-lag diffusion technique, D measured with sintered glass membranes (10, 11), and D measured by refractometry (12).

METHODS

Desorption kinetics

Lauric, myristic, and palmitic acids (Applied Science Laboratories, State College, Pa.), oleic acid (Hormel Institute, Austin, Minn.), and palmitoleic acid (K and K Laboratories, Plainview, N.Y.) were applied to the Langmuir trough in a hexane solution. Constant pressure–variable area measurements were obtained with a floating barrier and piston oils as previously described (1). Piston oils were castor oil, which generated 16.5 dynes/cm on neutral and alkaline subphases and 17–18.8 dynes/cm on an acid subphase, and tri-*m*-tolyl phosphate, which generated 9.5 dynes/cm on all subphases. The temperature was maintained at 25°C.

Subphase buffers at pH 10 and pH 11 and 0.1 ionic strength were prepared with sodium bicarbonate–sodium carbonate mixtures (13). Subphase buffers at pH 7 and pH 11 were also prepared by adding 0.01 M Tris to 0.1 M sodium chloride and adjusting the pH with either concentrated hydrochloric acid or concentrated sodium hydroxide (1, 8). Another alkaline subphase contained 0.1 N sodium hydroxide (pH 12.7). An acid subphase (Table 2) contained 0.01 N hydrochloric acid and 0.1 M sodium chloride (pH 2.1). All subphases contained 0.1 mM EDTA.

Time-lag diffusion

[1-^{14}C]Palmitic acid (0.04 mCi/mg, New England Nuclear, Boston, Mass.) was liquified by warming, introduced into a capillary sealed at one end, and attached to a thermometer with epoxy (Fig. 1). The capillary was then filled with buffer and introduced into a 50-ml buffer reservoir maintained at a constant temperature (Fig. 1). At stated time intervals, 0.5-ml aliquots were withdrawn from the buffer reservoir with a stainless steel needle inserted through glass tubing mounted in a fixed position in the buffer reservoir (Fig. 1). Radioactivity in the buffer was measured using a Packard Tri-Carb model 3380 liquid scintillation spectrometer. The volume of the buffer was corrected for prior sampling. The liquid scintillator consisted of the solvent toluene–Triton X-100–ethanol 4:2:1 (v/v) in which naphthalene (100 g/l), 2,5-diphenyloxazole (10 g/l) and 1,4-bis-2-(5-phenyloxazolyl)-benzene (0.3 g/l) were dissolved by stirring overnight.

The relative viscosity of the buffer was measured with an Ostwald viscometer.

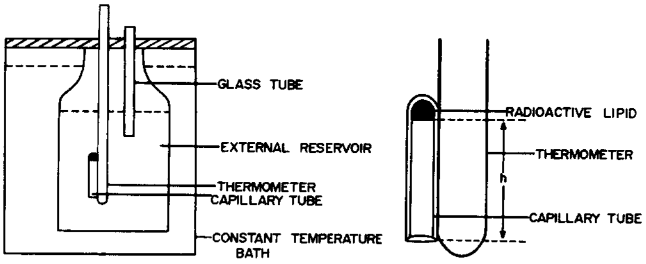

Fig. 1. Schematic diagram of apparatus for time-lag diffusion measurements.

RESULTS

Desorption kinetics

Data from typical desorption experiments are presented in Fig. 2. The fatty acid, pH, and subphase buffer used in these experiments were selected to provide a condensed monolayer (20.3 Å^2/molecule) when the piston oil exerted 16.5 dynes/cm and to provide a partially expanded monolayer (41.8 Å^2/molecule) when the piston oil exerted 9.5 dynes/cm. Surface areas for these unstable films were extrapolated from the desorption data (Eq. 1). Regions of linearity of log A with $\sqrt{t}$ preceded regions of linearity of log A with t in both experiments. All other desorption curves in this study displayed the same form, confirming the experimental observations of Ter Minassian-Saraga (3, 4). The experimental observations of Matuura et al. (9) were not reproduced in any desorption experiment.

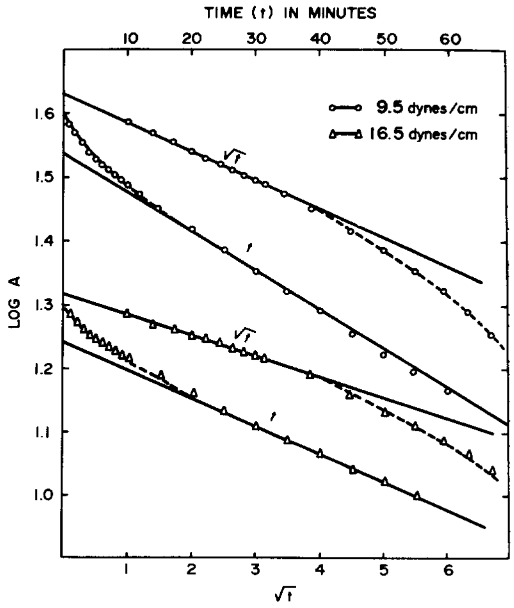

Fig. 2. The apparent surface area measured in Å^2/molecule, A, of a contracting palmitic acid monolayer measured as a function of time, t. Log A was plotted against both $\sqrt{t}$ and t at two specified surface pressures. Palmitic acid was spread on 0.01 M Tris–0.1 M sodium chloride adjusted to pH 9.0. The temperature was 25°C.

Equations for linear portions of the desorption curves were calculated by the method of least squares, and the desorption coefficients, K_i and K_s (Eqs. 1 and 2), were obtained from the slopes of these lines. K_i and K_s varied directly with surface pressure and with subphase pH, but the K_s/K_i ratio was independent of surface pressure, subphase pH, and buffer composition (Table 1). Ter Minassian-Saraga (3, 4) and Gershfeld (6) also found that desorption coefficients for fatty acids varied directly with surface pressure and subphase pH and that the K_s/K_i ratio was independent of these variables.

The subphase buffer had an unexpected effect on the desorption coefficients. At 9.5 dynes/cm and pH 10 or pH 11, K_i and K_s for palmitic acid spread on a sodium bicarbonate–sodium carbonate subphase were greater than K_i and K_s for palmitic acid spread on a Tris–sodium chloride subphase (Table 1). Furthermore, the desorption coefficients for palmitic acid spread on a sodium bicarbonate–sodium carbonate subphase at pH 10 were greater than the desorption coefficients for palmitic acid spread on a sodium hydroxide subphase at pH 12.7 even though the ionic strength was the same for both subphases (Table 1). Surface potential measurements (14) and infrared spectra (15) both suggest that the bicarbonate anion interacts with a fatty acid monolayer. Desorption studies provide additional evidence that the bicarbonate anion has an effect on the desorbing species.

TABLE 1. Desorption coefficients, K_i and K_s, for palmitic acid spread at two surface pressures on several alkaline subphases at 25°C

pH and Buffer[a]	K_i[b]	K_s[b]	K_s/K_i
	min$^{-0.5}$	*min*$^{-1}$	
A. 9.5 dynes/cm			
pH 10.1, $NaHCO_3$–Na_2CO_3 (4)[c]	0.104[d] ± 0.002	0.0133 ± 0.0003	0.128
pH 11.0, $NaHCO_3$–Na_2CO_3 (4)	0.119 ± 0.001	0.0143 ± 0.0009	0.120
pH 9.0, Tris–NaCl (8)	0.045 ± 0.003	0.0059 ± 0.0006	0.131
pH 10.1, Tris–NaCl (6)	0.080 ± 0.003	0.0098 ± 0.0003	0.122
pH 11.0, Tris–NaCl (6)	0.083 ± 0.001	0.0104 ± 0.0010	0.125
pH 12.7, NaOH (6)	0.087 ± 0.004	0.0109 ± 0.0006	0.125
B. 16.5 dynes/cm			
pH 9.0, Tris–NaCl (8)	0.032 ± 0.003	0.0045 ± 0.0005	0.141
pH 10.1, Tris–NaCl (8)	0.119 ± 0.005	0.0141 ± 0.0012	0.118
pH 11.0, Tris–NaCl (7)	0.145 ± 0.006	0.0179 ± 0.0007	0.123
Mean ± SD			0.126 ±0.007

[a] See Methods for detailed description of buffer.
[b] K_i and K_s were calculated from log A rather than ln A.
[c] Number of determinations is in parentheses.
[d] Means ± SD.

K_i and K_s were also obtained for lauric, myristic, palmitoleic, and oleic acids. Since K_s/K_i was independent of surface pressure and subphase composition, these experimental parameters were used to control the contraction rate and yield reproducible desorption coefficients. Regions of linearity of log A with $\sqrt{t}$ preceded regions of linearity of log A with t in these experiments. The data are summarized in Table 2.

Time-lag diffusion

Time-lag diffusion was developed by Daynes (16) and Barrer (17) for the diffusion of gases through rubber membranes. In this procedure, D was calculated from the relationship:

$$D = \frac{h^2}{6L} \qquad \text{Eq. 3}$$

where h is the thickness of the membrane and L is the lag period required to establish a gradient through the membrane. The rubber membrane used in gaseous diffusion is analogous to the capillary used in our time-lag diffusion apparatus (Fig. 1). The lag period required to establish a fatty acid gradient in this capillary was measured by the radioactivity in the buffer. The capillary was reused and, indeed, aging was required for the removal of small amounts of fatty acid which adhered to the sides of the capillary. A typical time-lag diffusion experiment is presented in Fig. 3.

D was measured for palmitic acid in a Tris–sodium chloride buffer at pH 9. 10 experiments yielded a mean of 5.7×10^{-6} cm^2/sec with a standard deviation of 2.3×10^{-6} cm^2/sec for D_{25}. The range in D_{25} was $3.1–9.8 \times 10^{-6}$ cm^2/sec; however, five D_{25} values were grouped at the lower end of this range and yielded a mean of 3.7 ×

TABLE 2. Desorption coefficients, K_i and K_s, for lauric, myristic, palmitoleic, and oleic acids at 25°C

pH and Buffer[a]	Surface Pressure	K_i[b]	K_s[b]	K_s/K_i
	dynes/cm	*min*$^{-0.5}$	*min*$^{-1}$	
Lauric acid				
pH 2.1, HCl–NaCl (6)[c]	17.0 18.5	0.054[d] ± 0.004	0.0087 ± 0.0008	0.161
Myristic acid				
pH 7.0, Tris–NaCl (6)	9.5	0.072 ± 0.001	0.0107 ± 0.0004	0.149
Palmitoleic acid				
pH 7.0, Tris–NaCl (6)	9.5	0.039 ± 0.003	0.005 ± 0.0002	0.128
Oleic acid				
pH 10.0, $NaHCO_3$–Na_2CO_3 (6)	16.5	0.096 ± 0.004	0.0101 ± 0.0006	0.105

[a] See methods for detailed description of buffer.
[b] K_i and K_s were calculated from log A rather than ln A.
[c] Number of determinations is in parentheses.
[d] Means ± SD.

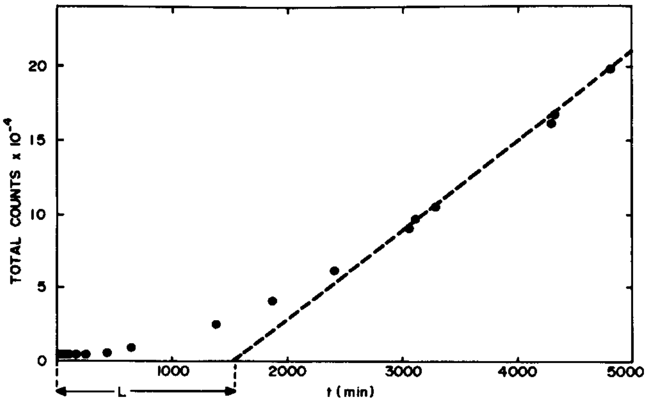

FIG. 3. Diffusion of sodium palmitate from a capillary measured as a function of time. The buffer contained 0.01 M Tris–0.1 M sodium chloride adjusted to pH 9.0. The temperature was 25°C.

10^{-6} cm²/sec with a standard deviation of 0.6×10^{-6} cm²/sec. A number of experimental errors were difficult to control in the time-lag diffusion procedure. The errors in D which were introduced by vibration, convection currents that resulted from temperature variations, and stirring that resulted from the sampling process all shortened the lag period and increased D. Consequently, it is probable that the lower grouped values more nearly represented D_{25} than the mean for all experiments.

DISCUSSION

A schematic diagram of the processes which result in the contraction of a monolayer is presented in Fig. 4. If ionization and desorption (steps *1* and *2* in Fig. 4) are fast quasi-equilibrium processes, diffusion through the unstirred layer (step *3a* in Fig. 4) is the initial rate-limiting step in the overall process. The rate-limiting step may be treated as diffusion into a semiinfinite medium from a plane of fixed concentration yielding the relationship (3, 4):

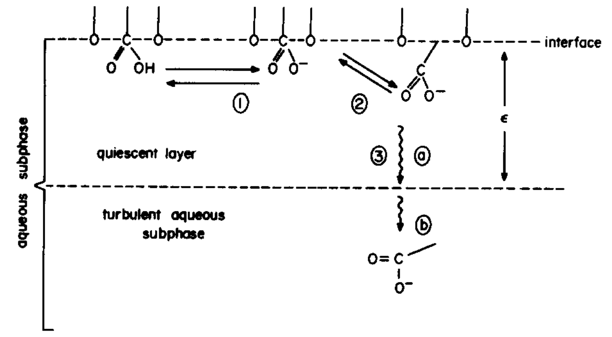

FIG. 4. Schematic diagram of the processes which result in monolayer contraction. *1*, ionization; *2*, desorption from the surface into an unstirred subphase layer of thickness ε; *3a*, diffusion through the unstirred layer; *3b*, escape from the unstirred layer.

$$\ln \frac{A}{A_0} = -2\frac{C_0}{\delta}\sqrt{\frac{D}{\pi}}\sqrt{t} \qquad \text{Eq. 4}$$

where A_0 is the area of the film at zero time, δ is the density of the monolayer in g/cm², and C_0 is the concentration of the diffusing species immediately adjacent to the monolayer in g/cm³. Eq. 1 is obtained when Eq. 4 is rearranged and differentiated with respect to $\sqrt{t}$:

$$-\frac{d \ln A}{d\sqrt{t}} = 2\frac{C_0}{\delta}\sqrt{\frac{D}{\pi}} = K_i \qquad \text{Eq. 5}$$

Our kinetic data supported this description of the first temporal phase in the desorption process rather than the description by Matuura et al. (9) in which ln A was linear with t. However, Matuura et al. (9) noted that the Ter Minassian-Saraga (3, 4) model for the first temporal phase in the desorption process may be a limiting case of their general desorption model, which is expressed in our notation by the equation:

$$\ln \frac{A}{A_0} = -\frac{C_0}{\delta}\left\{\frac{D}{k}\exp\left[\frac{k^2}{D}t\right]\operatorname{erfc}\left[\frac{k}{\sqrt{D}}\sqrt{t}\right] - \frac{D}{k} + 2\sqrt{\frac{D}{\pi}}\sqrt{t}\right\} \qquad \text{Eq. 6}$$

where k is the dissolution rate. As $k \rightarrow \infty$, the first two terms in Eq. 6 approach 0, and the equation reduces to Eq. 4. Furthermore, Patlak and Gershfeld (18) showed in a rigorous kinetic treatment of desorption that the time course of monolayer contraction was relatively insensitive to dissolution as a rate-limiting parameter and that linearity of ln A with $\sqrt{t}$ might be observed in cases where monolayer desorption was not an equilibrium process.

Ter Minassian-Saraga (3, 4) has suggested that a steady state develops in the second temporal phase of the desorption process. In the steady state, dissolution into the unstirred layer (step *2* in Fig. 4) equals escape from the unstirred layer (step *3b* in Fig. 4). A constant concentration gradient of desorbed molecules exists in the unstirred layer and, as a consequence, desorption is described in Eq. 2 where ln A is linear with t. Our kinetic data supported this description of the second temporal phase rather than the description by Matuura et al. (9), in which ln A was linear with $\sqrt{t}$.

The desorption models of Ter Minassian-Saraga (3, 4) and Matuura et al. (9) both estimate D for the desorbing species. In the Ter Minassian-Saraga model, D is obtained from the relationship:

$$\frac{K_s}{K_i} = \frac{\sqrt{\pi D}}{2\epsilon} \qquad \text{Eq. 7}$$

where ϵ, the width of the quiescent subphase layer adjacent to the monolayer (Fig. 4), was calculated as 0.12

cm from desorption measurements (3, 4). Ter Minassian-Saraga calculated two D values for lauric acid that differed from D for the laurate anion, which was measured by other techniques (Table 3). The D value for lauric acid which was calculated from our desorption data (Table 2) corresponded to D for the laurate anion (Table 3). These data supported the value which was calculated for ϵ by Ter Minassian-Saraga (3, 4). Lower values for ϵ have been proposed by other investigators (19).

An empirical approximation used in diffusion studies (20) suggests that D is inversely proportional to the square root of molecular weight, $\sqrt{M}$, for compounds in a homologous series, and as a consequence $D\sqrt{M}$ is a constant. This constant was calculated for long-chain fatty acids or their anions (Table 3). Laurate data of McBain and Liu (10), caprylate and laurate data of Lamm and Högberg (12), and lauric and myristic acid data from the present study all yielded a similar value for $D\sqrt{M}$ (Table 3). Lauric acid data of Ter Minassian-Saraga were in less close agreement (Table 3). D values for palmitoleic acid, palmitate, and oleate which were calculated in the present study and the D value for oleate which was obtained by McBain (11) decreased more rapidly with increasing molecular weight than was expected for a homologous series (Table 3). Both McBain and Liu (10) and Lamm and Högberg (12) found that D was concentration dependent, and indeed Lamm and Högberg (12) suggested that laurate at higher concentrations diffused as a micelle. The lower D values found in the present study by desorption and time-lag techniques could be explained by the diffusion of higher fatty acids as small aggregates averaging two to four molecules in size because these aggregates yielded the expected $D\sqrt{M}$ value (Table 3). It is apparent that a tendency to aggregate may complicate the measurement of D for higher fatty acids in dilute aqueous solutions. Finally, the constant $D\sqrt{M}$ which was calculated from the D values for short-chain carboxylic acids (21) ranged from 83 to 96. The constant $D\sqrt{M}$ which was calculated from the D values for long-chain fatty acids ranged from 100 to 118 (Table 3). This difference may be explained by the greater relative hydration of the short-chain carboxylic acids.

TABLE 3. Diffusion coefficient at 25°C (D), and the relationship between D and the square root of molecular weight ($\sqrt{M}$)

Compound	Normality	D	$\sqrt{M}$	$D\sqrt{M}$
		10^{-6} *cm²/sec*		
A. Sintered glass membrane: McBain and Liu (10)				
Laurate	0.025	8.1	14.1	114
B. Sintered glass membrane: McBain (11)				
Oleate	0.025	5.3	16.8	89
C. Refractometry: Lamm and Högberg (12)				
Caprylate	0.01	8.4[a]	12	101
Laurate	0.01	8.0[a]	14.1	113
D. Desorption: Ter Minassian-Saraga (3, 4)				
Lauric acid		6.7[b]	14.1	94
Lauric acid		8.7[b]	14.1	123
E. Desorption: this study				
Lauric acid		7.9 ± 0.6	14.1	111
Myristic acid		6.6 ± 0.3	15.1	100
(Palmitoleic acid)$_2$		4.9 ± 0.3	22.5	110
(Palmitate)$_2$		4.8 ± 0.6	22.6	108
(Oleate)$_4$		3.3 ± 0.2	33.6	111
F. Time-lag: this study				
(Palmitate)$_4$		3.7 ± 0.6	31.9	118
G. Desorption: Matuura et al. (9)				
Myristic acid		14.0	15.1	211

[a] Converted from 20°C values by the Stokes-Einstein relationship.

[b] Converted from 19°C values by the Stokes-Einstein relationship.

In spite of the difficulties that are involved in the measurement of D, the value that Matuura et al. (9) obtained for myristic acid was much too high (Table 3). These investigators suggested that their value for D was increased by mechanical vibration even though their equations were derived for a quiescent semiinfinite medium. It is apparent that the Ter Minassian-Saraga model provides a more adequate description of the desorption process for fatty acid monolayers.

In the Ter Minassian-Saraga model (Eq. 5), the initial desorption coefficient, K_t, is directly proportional to the concentration of the diffusing species immediately adjacent to the monolayer, C_0. Since this model is based on the requirement that ionization and initial desorption are fast quasi-equilibrium processes, C_0 may be related to the degree of ionization of the monolayer. K_t may, therefore, be useful in the estimation of apparent surface pK_a, and this application of the desorption process will be presented in a subsequent study.

This study was supported in part by research grant GM-09506 from the National Institute of General Medical Sciences.

Manuscript received 12 May 1972; accepted 8 September 1972.

REFERENCES

1. Heikkila, R. E., D. W. Deamer, and D. G. Cornwell. 1970. Solution of fatty acids from monolayers spread at the air–water interface: identification of phase transformations and the estimation of surface charge. *J. Lipid Res.* **11:** 195–200.
2. Motomura, K., A. Shibata, M. Nakamura, and R. Matuura. 1969. Fatty acid monolayers in the expanded state. II. The effect of compression velocities. *J. Colloid Interface Sci.* **29:** 623–628.
3. Ter Minassian-Saraga, L. 1955. Études de l'adsorption et de la désorption aux surfaces liquides. *J. Chim. Phys.* **52:** 181–200.
4. Ter Minassian-Saraga, L. 1956. Recent work on spread monolayers, adsorption and desorption. *J. Colloid Sci.* **11:** 398–418.
5. Gershfeld, N. L., and C. S. Patlak. 1966. Activity coeffi-

cients of monomolecular films from desorption studies. *J. Phys. Chem.* **70:** 286–288.

6. Gershfeld, N. L. 1968. Cohesive forces in monomolecular films at an air–water interface. *Advan. Chem. Ser.* **84:** 115–130.
7. Zografi, G., R. Verger, and G. H. De Haas. 1971. Kinetic analysis of the hydrolysis of lecithin monolayers by phospholipase A. *Chem. Phys. Lipids.* **7:** 185–206.
8. Patil, G. S., R. H. Matthews, and D. G. Cornwell. Effect of ionization and cation selectivity on the expansion of stearic acid monolayers. *J. Lipid Res.* **13:** 574–579.
9. Matuura, R., K. Sekita, and K. Motomura. 1969. The desorption of monolayers of fatty acid. *In* Chimie, Physique et Applications Pratiques des Agents de Surface. Vol. 2. Ediciones Unidas, Barcelona. 375–381.
10. McBain, J. W., and T. H. Liu. 1931. Diffusion of electrolytes, non-electrolytes and colloidal electrolytes. *J. Amer. Chem. Soc.* **53:** 59–74.
11. McBain, M. E. L. 1933. The diffusion of colloidal electrolytes; sodium oleate. *J. Amer. Chem. Soc.* **55:** 545–551.
12. Lamm, O., and H. Högberg. 1940. Refractometrische Messung der freien Diffusion der Seifen in wässeriger Lösung. *Kolloid Z.* **91:** 10–19.
13. Long, C. 1961. Biochemists' Handbook. Van Nostrand, New York.
14. Goddard, E. D., S. R. Smith, and O. Kao. 1966. Monolayer properties of fatty acids. II. Behenic acid. *J. Colloid Interface Sci.* **21:** 320–330.
15. Bagg, J., M. D. Haber, and H. P. Gregor. 1966. Composition of stearic and behenic acid monolayers from sodium-containing substrates. *J. Colloid Interface Sci.* **22:** 138–143.
16. Daynes, H. A. 1920. The process of diffusion through a rubber membrane. *Proc. Roy. Soc. Ser. A.* **97:** 286–307.
17. Barrer, R. M. 1939. Permeation, diffusion and solution of gases in organic polymers. *Trans. Faraday Soc.* **35:** 628–643.
18. Patlak, C. S., and N. L. Gershfeld. 1967. A theoretical treatment for the kinetics of monolayer desorption from interfaces. *J. Colloid Interface Sci.* **25:** 503–513.
19. Davies, J. T., and E. K. Rideal. 1963. Interfacial Phenomena. Academic Press, New York. 181.
20. Jacobs, M. H. 1967. Diffusion Processes. Springer-Verlag, New York. 13.
21. Bidstrup, D. E., and C. J. Geankoplis. 1963. Aqueous molecular diffusivities of carboxylic acids. *J. Chem. Eng. Data.* **8:** 170–173.